The Astrophysical Journal, 834:200 (11pp), 2017 January 10 doi:10.3847/1538-4357/834/2/200

DETECTING TRIPLE SYSTEMS WITH GRAVITATIONAL WAVE OBSERVATIONS

Yohai Meiron[1], Bence Kocsis[1], and Abraham Loeb[2]
[1] Institute of Physics, Eötvös University, Pázmány P. s. 1/A, Budapest, 1117, Hungary
[2] Center for Astrophysics, 60 Garden Street, MS-51, Cambridge, MA 02138, USA
Received 2016 April 19; revised 2016 October 13; accepted 2016 November 25; published 2017 January 13

ABSTRACT

The Laser Interferometer Gravitational Wave Observatory (LIGO) has recently discovered gravitational waves (GWs) emitted by merging black hole binaries. We examine whether future GW detections may identify triple companions of merging binaries. Such a triple companion causes variations in the GW signal due to: (1) the varying path length along the line of sight during the orbit around the center of mass; (2) relativistic beaming, Doppler, and gravitational redshift; (3) the variation of the "light"-travel time in the gravitational field of the triple companion; and (4) secular variations of the orbital elements. We find that the prospects for detecting a triple companion are the highest for low-mass compact object binaries which spend the longest time in the LIGO frequency band. In particular, for merging neutron star binaries, LIGO may detect a white dwarf or M-dwarf perturber at a signal-to-noise ratio of 8, if it is within 0.4 $R_\odot$ distance from the binary and the system is within a distance of 100 Mpc. Stellar mass (supermassive) black hole perturbers may be detected at a factor 5 $\times$ ($10^3\times$) larger separations. Such pertubers in orbit around a merging binary emit GWs at frequencies above 1 mHz detectable by the *Laser Interferometer Space Antenna* in coincidence.

Key words: black hole physics – gravitational waves – stars: kinematics and dynamics

1. INTRODUCTION

The Laser Interferometer Gravitational Wave Observatory[3] (LIGO) has recently announced the detection of gravitational waves (GWs) from two merging black hole (BH) binaries GW150914 (Abbott et al. 2016a) and LVT151012 (Abbott et al. 2016c), opening a new era of GW astronomy. With the further development of GW detectors including Virgo[4] and KAGRA[5], merging compact object binaries are expected to be detected regularly at a rate of several per day within a distance of 7 Gpc (Abbott et al. 2016b). In this work, we examine whether the presence of a triple companion could be detected by measuring the GW signal of the merging binary.

We consider a hierarchical triple system, where two stellar mass compact objects form an "inner binary," with a triple companion at a large distance compared to the inner binary's orbital separation. The inner binary's orbit shrinks due to the GW radiation reaction while it is orbiting the triple system's center of mass (see Figure 1). This orbital motion due to the third companion causes modifications to the GW signal due to a time dependent change in the: (1) path length to the observer, (2) relativistic Doppler and gravitational redshift, and (3) "light"-travel time of the GW signal as it crosses the gravitational field of the companion. These effects are well studied in pulsar binaries, in which the pulsar orbits another compact object, known respectively as Roemer, Einstein, and Shapiro delays. Here, the pulsar is replaced by the GW source, the merging inner binary, and instead of timing the radio pulses we measure the distortion of the GW waveform relative to a theoretical waveform corresponding to an isolated (i.e., unperturbed) inspiraling BH binary. Furthermore, the relativistic beaming of the orbit of the GW source provides an amplitude modulation, and the triple companion has a dynamical influence which drives variations of the intrinsic orbital elements of the GW-emitting binary. In this study, we examine whether any of these effects may be detected in a GW signal to unveil the presence of a third object in the vicinity of the GW source.

Hierarchical triples are common in astrophysics. More than 40% of stellar systems with a white dwarf (WD) and a short period binary form triples, and generally 42 $\pm$ 5% of massive stars brighter than 10 mag are in triples (Tokovinin 1997; Pribulla & Rucinski 2006; Pfuhl et al. 2014). Thus, unless the BHs receive a substantial birth kick at their formation[6], they may also be expected to commonly reside in triple systems. Only one compact object triple is known to date: a close NS +WD binary orbited by another WD, which was found in the Galactic disk (Ransom et al. 2014).

The likelihood of finding a triple companion may be different among the different environments in which compact object mergers occur: dense dynamical stellar systems such as globular clusters (Portegies Zwart & McMillan 2000; Wen 2003; O'Leary et al. 2006; Antonini et al. 2014; O'Leary et al. 2016; Rodriguez et al. 2016) or galactic nuclei (O'Leary et al. 2009; Kocsis & Levin 2012), active galactic nuclei (AGNs; Bartos et al. 2016; Stone et al. 2016), galactic field mergers catalyzed by special modes of stellar evolution (Belczynski et al. 2016; de Mink & Mandel 2016; Mandel & de Mink 2016; Marchant et al. 2016) or the first stars (Kinugawa et al. 2014, 2016; Dvorkin et al. 2016; Hartwig et al. 2016; Inayoshi et al. 2016), cores of massive stars (Reisswig et al. 2013; Loeb 2016; Woosley 2016), or dark matter halos comprised of primordial BHs (Bird et al. 2016; Clesse & García-Bellido 2016; Sasaki et al. 2016). Close compact object triples may form through common envelope evolution in galaxies (Tauris & van den Heuvel 2014). Alternatively, they may form dynamically in dense stellar environments where many of the compact object mergers

[3] http://www.ligo.org/
[4] http://www.virgo-gw.eu/
[5] http://gwcenter.icrr.u-tokyo.ac.jp/en/

[6] Only small birth kicks are expected in many cases (Amaro-Seoane & Chen 2016)

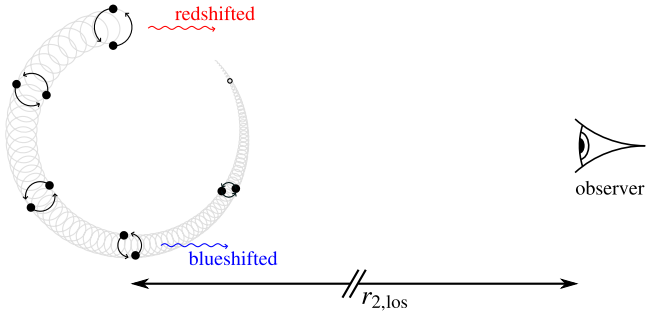

Figure 1. Schematic illustration of the triple systems under consideration (not to scale). The gray curve represents the trajectory of the inspiraling "inner binary." The inner binary separation a_1 shrinks because of gravitational wave emission, while its center of mass orbits around the triple system's center of mass forming an "outer binary" with separation $a_2 \gg a_1$ (not shown). The gray curve starts when the inner binary's gravitational wave frequency enters the detector's sensitive range, and ends when the inner binary reaches the innermost stable circular orbit and coalesces. Depending on the three masses and a_2, the inner binary may complete thousands of inner orbits and multiple revolutions around the triple's center of mass while in the LIGO/Virgo band, whereas for others it completes only a small fraction of an outer orbit (see Equation (4)).

detectable by LIGO/Virgo may originate (Portegies Zwart & McMillan 2000; Ivanova et al. 2005; Samsing et al. 2014; O'Leary et al. 2016; Rodriguez et al. 2016). In fact, the triple companion may be the cause of the compact object merger itself by driving eccentricity oscillations, the so-called Kozai–Lidov effect (Blaes et al. 2002; Miller & Hamilton 2002; Wen 2003; Katz et al. 2011; Antonini & Perets 2012; Naoz et al. 2013a; Seto 2013; Antognini et al. 2014; Antonini et al. 2014; Naoz 2016).

The possibility of measuring the influence of a massive perturber for the *Laser Interferometer Space Antenna* (*LISA*) extreme mass ratio inspirals (EMRIs) was discussed by Yunes et al. (2011b). Schnittman (2010) showed that a corotation resonance may drag test particles close to the merger of inspiraling intermediate-mass ratio or EMRI BH binaries, which if tidally disrupted, may lead to an electromagnetic counterpart (see also Yamada et al. 2015 for generalizations to arbitrary mass ratios, Seto & Muto 2011 for other mean motion resonances, and Zhou et al. 2016 for the collinear triple configuration for the scalar-tensor theory of gravity). Galaviz & Brügmann (2011) examined post-Newtonian dynamical effects associated with hierarchical triple systems and found that the triple companion affects the octupole GW radiation waveform. Furthermore, Kocsis (2013) showed that a supermassive BH in the vicinity of a LIGO/Virgo source may result in a GW echo detectable with LIGO/Virgo if the primary signal has a high signal-to-noise ratio (S/N).

More generally, detecting the astrophysical environment of GW sources may be important for understanding their origin. A shift of the BH ringdown frequency could be used to look for a Planck-density firewall near the horizon with *LISA* and perhaps also with LIGO/Virgo (Barausse et al. 2014), if it exists. The influence of an embedding gaseous disk during a GW inspiral may be detected with *LISA* (Barausse & Rezzolla 2008; Kocsis et al. 2011; Yunes et al. 2011a) or with the aid of electromagnetic observations (Kocsis et al. 2006; Kocsis & Loeb 2008; Alic et al. 2012; Bode et al. 2012; Farris et al. 2012; Giacomazzo et al. 2012; Kocsis et al. 2012; Noble et al. 2012; McKernan et al. 2013; Gold et al. 2014b; Farris et al. 2015). A double jet may also be characteristic of a binary merger in a gaseous environment (Palenzuela et al. 2010). Similar effects may be detected for pulsar timing array GW sources (Kocsis & Sesana 2011; Tanaka & Haiman 2013; Generozov & Haiman 2014; Gold et al. 2014a; Roedig et al. 2014). The measurement of the interaction of GWs with matter is expected to be practically very challenging (Kocsis et al. 2008; Li et al. 2012; McKernan et al. 2014).

In this work, we quantify the parameter space of triple companion mass and separation where its effect on the GW signal may be detected with Advanced LIGO/Virgo. In Section 2, we list the basic equations that define the characteristics of the triple system and the GWs. In Section 3, we review the S/N of detecting the perturbation and the significance of the GW phase shift. In Section 4, we analytically estimate the order of magnitude of the GW phase shift for the various physical effects as a function of the triple's physical parameters and present numerical results for the detectability of the third object. Finally, in Section 5, we discuss the implications of triple detections using LIGO/Virgo and *LISA*.

We use geometrized units with $G = c = 1$. To change from mass to distance or time units, one should multiply all mass terms by G/c^2 or G/c^3, respectively.

2. CHARACTERISTICS OF THE TRIPLE

We assume a hierarchical triple of mass (m_a, m_b, m_c) which consists of an "inner binary" and an "outer binary" labeled by index 1 and 2, respectively. The inner binary is comprised of (m_a, m_b), with total mass $M_1 = m_a + m_b$, symmetric mass ratio $\eta_1 = m_a m_b/(m_a + m_b)^2$, and separation a_1 which shrinks as a function of time due to GW radiation reaction. The outer binary consists of the center of mass of the inner binary of mass M_1 and the outer perturber m_c with total mass $M_2 = m_a + m_b + m_c$, symmetric mass ratio $\eta_2 = (m_a + m_b)\, m_c/(m_a + m_b + m_c)^2$, and separation a_2 which may also slowly shrink due to the GW radiation reaction. The orbital angular frequency for both binaries $i = (1, 2)$ is to leading order

$$\Omega_i = M_i^{-1}\left(\frac{a_i}{M_i}\right)^{-3/2}. \quad (1)$$

For circular orbits, the comoving GW frequency is twice the orbital frequency, $f_i = \Omega_i/\pi = \pi^{-1}(a_i/M_i)^{-3/2}M_i^{-1}$.

As the binaries emit GWs their separations decrease and GW frequencies increase. For circular binaries, the time to merger from given a_i or f_i is

$$t_{i,\rm merge} = \frac{5}{256}\frac{a_i^4}{\eta_i M_i^3} = 5(8\pi f_i)^{-8/3}\mathcal{M}_i^{-5/3}, \quad (2)$$

where $\mathcal{M}_i = \eta_i^{3/5}M_i$ is the chirp mass of the ith binary. The inspiral waveform ends[7] at $a_{i,\rm ISCO} = 6\,M_i$ BH binary or a maximum GW frequency $f_{i,\rm ISCO} = \pi^{-1}6^{-3/2}M_i^{-1}$, which is around $\sim$1.6 kHz for neutron star–neutron star (NS–NS) binaries.

We label the orbital phase[8] with ϕ_i for the two binaries, which satisfy $\Omega_i = d\phi_i/dt$. The GW phase Φ_i satisfies $d\Phi_i/dt = f_i$ and so in a comoving frame with the center of

[7] For maximally spinning BH binaries, $a_{i,\rm ISCO} = 1$–$9\,M_i$, depending on the direction of the spin.

[8] More specifically the true anomaly, but we restrict to circular orbits unless mentioned otherwise.

mass of the inner binary,

$$\Phi_1 = 2\phi_1 = 2\phi_{1,0} + 2(8\pi f_1 \mathcal{M}_1)^{-5/3} = 2\phi_{1,0} + 2\left(\frac{|t-t_0|}{5\mathcal{M}_1}\right)^{5/8}, \quad (3)$$

where $f_1 = \Omega_1/\pi = d\Phi_1/dt$ is the comoving GW frequency of the inner binary, t is the comoving time, t_0 is time of coalescence of the inner binary, and $\phi_{1,0}$ is the orbital phase of the coalescence. Note that the GW phase accumulates mainly near the minimum observation frequency $f_{\rm min}$.

Similar equations hold for the outer binary. If the observation is short relative to $t_{2,\rm merge}$, we may approximate Ω_2 with a constant and

$$\phi_2 = \phi_{2,0} + \Omega_2|t-t_0|, \quad (4)$$

where $\phi_{2,0}$ is the orbital phase at t_0. The orbital phase completed by the outer binary during which the GW frequency of the inner binary is above $f_{\rm min}$ is

$$\phi_{2,\rm tot} = \Omega_2 t_{1,\rm merge} = 3.5\,\bar{f}_{\rm min}^{-8/3}(4\eta_1)\bar{M}_1^{-5/3}\bar{M}_2^{1/2}\bar{a}_2^{-3/2}, \quad (5)$$

where barred quantities are measured in some specific units: mass parameters are in $M_\odot = 2\times10^{33}$ g, distances such as a_2 are in $R_\odot = 7\times10^{10}$ cm, and frequencies such as $f_{\rm min}$ are measured in units of 10 Hz (the minimum detectable GW frequency for Advanced LIGO).

The line of sight (LOS) distance to the center of mass of the inner binary is

$$r_{1,\rm los} = r_{2,\rm los} - \frac{m_{\rm c}}{M_2}a_2\sin\iota_2\cos\phi_2, \quad (6)$$

where we assume that the center of mass of the outer binary is fixed at $r_{2,\rm los}$, and ι_2 is the angle between the orbital angular momentum vector of the outer binary and the LOS.[9] The magnitude of the orbital velocity of the center of mass of the inner binary is

$$v_1 = \frac{m_{\rm c}}{M_2}a_2\Omega_2 = \frac{m_{\rm c}}{M_2}\left(\frac{a_2}{M_2}\right)^{-1/2}, \quad (7)$$

which is less than 0.03 (of the speed of light) if $a_2 \geqslant 10^3 M_2$, the case we are considering here.

We note that the triple must be hierarchical and the inner binary must not be disrupted by the outer binary for these estimates. The Eggleton & Kiseleva (1995) stability criterion for circular orbits is

$$\frac{a_2}{a_1} \gtrsim Y_0 \equiv 1 + \frac{3.7}{q_2^{1/3}} + \frac{2.2}{1+q_2^{1/3}} + \frac{1.4}{q_1^{1/3}}\frac{q_2^{1/3}-1}{q_2^{1/3}+1}, \quad (8)$$

where $q_1 = m_{\rm a}/m_{\rm b} \geqslant 1$ and $q_2 = (m_{\rm a}+m_{\rm b})/m_{\rm c}$ are the mass ratio of the inner and outer binary, respectively. Furthermore, if the outer object is not a BH or an NS, it needs to be beyond the tidal disruption radius to form a stable triple

$$a_2 \geqslant r_{\rm tidal} = \left(\frac{3M_1}{4\pi\rho_{\rm c}}\right)^{1/3} = 1.2\,R_\odot\bar{M}_1^{1/3}\bar{\rho}_{\rm c}^{-1/3} \quad (9)$$

where $\bar{\rho}_{\rm c}$ is the density of the outer object in units of g cm^{-3}. Note that for WDs, $\rho \sim 10^6$ g cm^{-3}, implying that $r_{\rm tidal} \sim 0.01\bar{M}_1^{1/3}\,R_\odot$.

A relativistic triple system which is hierarchical and stable may not have been so in the past. By applying the Peters (1964) formula for orbital decay to both inner and outer binaries, we find that the ratio of semimajor axis ratio evolves according to[10]

$$\frac{a_2}{a_1} = \left[\kappa^4 + \left(\frac{a_{2,0}}{a_1}\right)^4\right]^{1/4}, \quad (10)$$

where $a_{2,0}$ is the outer binary separation at the merger of the inner binary, a_1 is a monotonically decreasing function of time (given by Peters 1964), and

$$\kappa^4 = \frac{\eta_2 M_2^3}{\eta_1 M_1^3} = \frac{(m_{\rm a}+m_{\rm b}+m_{\rm c})m_{\rm c}}{m_{\rm a}m_{\rm b}}. \quad (11)$$

The purpose of this "backward integration" is to put an upper limit on the possible past lifetime of a triple that LIGO/Virgo may detect. Under the assumption that the inner binary merges first[11], the ratio a_2/a_1 is monotonically increasing with time, meaning that the triple system becomes more stable as both inner and outer components lose orbital energy to GWs. Thus, one may ask whether there was some point in time that the system was dynamically unstable, according to some criterion such as Equation (8). Depending on $m_{\rm c}$, κ may be arbitrarily small or large. In case $\kappa \geqslant Y_0$, the triple remains dynamically stable forever in the past of the inner binary merger, approaching an asymptotic self-similar stationary state[12] with $a_2/a_1 \approx \kappa$. Otherwise if $\kappa < Y_0$, then the triple becomes dynamically unstable in a time

$$t_{\rm stable} = 6.0\times10^8\ {\rm year}(4\eta_1)^{-1}\bar{M}_1^{-3}(Y_0^4-\kappa^4)^{-1}(\bar{a}_{2,0})^4 \quad \text{if } \kappa < Y_0 \quad (12)$$

before the merger of the inner binary. The characteristic past lifetime or residence time of a circular triple with $a_2 \sim a_{2,0}$ is the minimum of $t_{\rm stable}$ and $t_{2,\rm merge}$ (Equation (2)). The likelihood of finding a triple companion at $a_{2,0}$ is proportional to this characteristic timescale. We note that these estimates are significantly modified for eccentric triples.

3. DETECTING GW PERTURBATIONS

For an inspiraling source at a fixed distance[13] D and a random[14] source sky position and orientation, the detected

[9] If the center of mass of the merging binary moves at a fixed LOS velocity, v_1, then the GW signal changes only by rescaling all mass parameters by a Doppler factor $(1+v_2)$, and rescaling the source distance due to relativistic beaming.

[10] We assume that the binaries evolve independently from one another and only due to GW emission.

[11] Under arbitrary initial conditions, the outer binary may catch up with the inner binary before it merges, disrupting the hierarchical structure and stability.

[12] In the limit $a_{2,0} \approx 0$, the triple evolves self-similarly down all the way to the innermost stable circular orbit (ISCO) of either binary.

[13] If the source is at a cosmological redshift z, D is the luminosity distance and the mass parameters must be multiplied by $(1+z)$.

[14] The prefactor assumes a root-mean-square average of the detected GW strain in a single LIGO-type detector for isotropically chosen source sky position and orientation. We neglect the effects of a peculiar velocity and weak lensing here (Kocsis et al. 2006).

dimensionless strain is

$$h(t) = \frac{16}{5}\frac{\eta_1 M_1}{D} f(t)^{2/3}\cos[\Phi(t)], \quad (13)$$

where $\Phi(t)$ is given by Equation (3) and $f = d\Phi/dt$, and the one-sided Fourier transform in the stationary phase approximation is to leading (2.5 post-Newtonian) order (Cutler & Flanagan 1994)

$$\tilde{h} = \frac{\mathcal{M}_1^{5/6}}{\pi^{2/3}\sqrt{30}\,D} f^{-7/6} e^{i\Psi(f)}, \quad (14)$$

where the Fourier phase above is

$$\begin{aligned}\Psi(f) &= 2\pi f t(f) - \Phi(f) - \frac{\pi}{4} \\ &= 2\pi f t_0 - 2\phi_{1,0} + \frac{3}{4}(8\pi\mathcal{M}_1 f)^{-5/3} - \frac{\pi}{4}. \end{aligned} \quad (15)$$

In the second line we have used Equation (3) for the inner binary, where $\phi_{1,0}$ is the orbital phase at merger, and $t(f) = t_0 - t_{1,\mathrm{merge}}(f)$ given by Equation (2).

We discuss the detectability of a GW perturbation following Kocsis et al. (2011). To detect a perturbation to the GW signal, δh, the S/N of the perturbation

$$\begin{aligned}\left\langle \frac{S_{\mathrm{pert}}^2}{N^2} \right\rangle &= 4\int_{f_{\min}}^{f_{\max}} \frac{|\delta\tilde{h}|^2}{S_n} df = 8\int_{f_{\min}}^{f_{\max}} \frac{|\tilde{h}|^2(1-\cos\delta\Psi)}{S_n} df \\ &\approx 4\int_{f_{\min}}^{f_{\max}} \frac{|\tilde{h}|^2}{S_n}\delta\Psi^2 df \end{aligned} \quad (16)$$

must exceed a given detection threshold, typically S/N $\gtrsim 8$ for a false alarm probability of 0.02 (Abbott et al. 2016a). Here S_n is the one-sided mean-square spectral noise density with units of $1/\mathrm{Hz}$ characteristic of the instrument (Shoemaker 2015), and for Advanced LIGO $f_{\min} \sim 10\,\mathrm{Hz}$, $f_{\max}$ is the maximum frequency set by the coalescence, and $\delta\Psi$ is the dephasing caused by the perturbation. In the second equality in Equation (16), we assumed that the GW signal h is perturbed by a GW phase, $\delta\Phi$, which leads to a corresponding Fourier phase shift $\delta\Psi$ (Equation (15)), so $\delta\tilde{h} = \tilde{h}e^{i\delta\Psi} - \tilde{h}$, and in the third equality we expanded to second order in $\delta\Psi$.

The conclusion from Equations (15) and (16) is that the perturbation may be detected if the original unperturbed GW source has S/N $\gtrsim 8$ and the perturbation generates a phase shift $\delta\Phi \gtrsim 1$ rad.[15] Note that the phase shift is an intrinsic property of the perturbation, independent of the source distance from the Earth.

Figure 2 shows the dimensionless spectral amplitude of the signal $2f\tilde{h}$ and the residual $2f\delta\tilde{h}$ in blue and red lines, respectively, and the root-mean-square noise per logarithmic frequency bin ($\sqrt{fS_n}$, black curve, Shoemaker 2015). Specifically, the red curve shows the perturbation of the signal due to the leading order effect of a third companion, the Doppler phase, discussed in Section 4.1 below. The cases shown are (left panel) two NSs inspiraling in the presence of a WD, and (right panel) two BHs inspiraling in the presence of a third BH of the same mass (right panel). The ratio of the blue and the black curves integrated over $\ln f$ gives the S/N.

[15] $\delta\Phi$ may be somewhat smaller if the unperturbed signal has S/N $\gg 8$.

4. PERTURBATIONS OF GWS IN TRIPLE SYSTEMS

In the following subsections, we calculate the GW phase shift corresponding to the various physical effects related to the triple companion.

4.1. Doppler Shift

In analogy with signals emitted by pulsars in binary systems, we expect the largest perturbation in the GW signal to be caused by the variation of the LOS distance to the source, which leads to a shift in the arrival time of pulses called Roemer (or Rømer) delay. We are interested in comparing the GW signal of the actual inspiraling inner binary orbiting in a hierarchical triple system (the *source*), and a fictitious isolated inspiraling binary (the *reference system*). This reference system has a constant center of mass (LOS) velocity $v_{1,\mathrm{ref}}$ and merges at the same time as the source, where the position, velocity, and phase are set to equal those of the source. The GW phase difference is

$$\delta\Phi_{\mathrm{D}} = \Phi[t_{\mathrm{em}} - r_{1,\mathrm{los}}(t_{\mathrm{em}})] - \Phi[(1-v_{1,\mathrm{ref}})t_{\mathrm{em}} - r_{1,\mathrm{los}}(t_0)], \quad (17)$$

where $\Phi(t)$ is given by Equation (3), t_{em} is time of emission (retarded time), $r_{1,\,\mathrm{los}}$ is the LOS distance given by Equation (6), and t_0 is the time of merger. In the following calculations we set $v_{1,\mathrm{ref}}$ to be the value of the LOS velocity at merger, $v_{1,\mathrm{ref}} = \dot{r}_{1,\mathrm{los}}(t_0)$.

Before showing the numerical result for Equation (17) for various triple-system parameters, it is useful to get a rough estimate of the order of magnitude of this effect analytically. Yunes et al. (2011b) examined the GW phase shift when the outer binary orbital phase is small enough that the term $r_{1,\,\mathrm{los}}(t_{\mathrm{em}})$ may be approximated by its quadratic Taylor series at t_0

$$r_{1,\mathrm{los}}(t_{\mathrm{em}}) \approx r_{1,\mathrm{los}}(t_0) + v_{1,\mathrm{los}}t_{\mathrm{em}} + \frac{1}{2}\dot{v}_{1,\mathrm{los}}t_{\mathrm{em}}^2, \quad (18)$$

where the velocity and acceleration may be calculated from Equation (6) to be $v_{1,\mathrm{los}} = -m_{\mathrm{c}}M_2^{-1}a_2\Omega_2\sin\iota_2\sin\phi_2$ and $\dot{v}_{1,\mathrm{los}} = -m_{\mathrm{c}}M_2^{-1}a_2\Omega_2^2\sin\iota_2\cos\phi_2$. Setting $v_{1,\mathrm{ref}} = v_{1,\mathrm{los}}(t_0)$, the phase difference $\delta\Phi_{\mathrm{D}}$ is zero at time t_0 due to the definition of $\Phi(t)$ in Equation (3), and it accumulates during the GW observation for earlier times before merger. After expanding both $\Phi(t)$ terms in Equation (17) in a series to first order in its argument around the point $t = r_{1,\mathrm{los}}(t_0) + v_{1,\mathrm{los}}t_{\mathrm{em}}$ using Equation (18), the first two terms drop out in Equation (18) and only the term proportional to $\dot{v}_{1,\mathrm{los}}$ remains in the phase difference. We get that the total Doppler phase shift during the full LIGO measurement from GW frequency $f_{\min}$ to merger is

$$\begin{aligned}\delta\Phi_{\mathrm{D}} &\approx \frac{1}{2}\dot{\Phi}\dot{v}_1 t_{1,\mathrm{merge}}^2 = \frac{1}{2}f_{\min}\,\dot{v}_1 t_{1,\mathrm{merge}}^2 \\ &= 890\,\bar{f}_{\min}^{-13/3}(4\eta_1)^{-2}\bar{M}_1^{-10/3}\bar{m}_{\mathrm{c}}\bar{a}_2^{-2}\sin\iota_2\cos\phi_2, \end{aligned} \quad (19)$$

where we used Equation (2) for $t_{1,\mathrm{merge}}$. The quantities denoted by a bar are in physical units and are defined under Equation (5). This approximation assumes that ϕ_2 is approximately constant during the measurement. Let us examine where

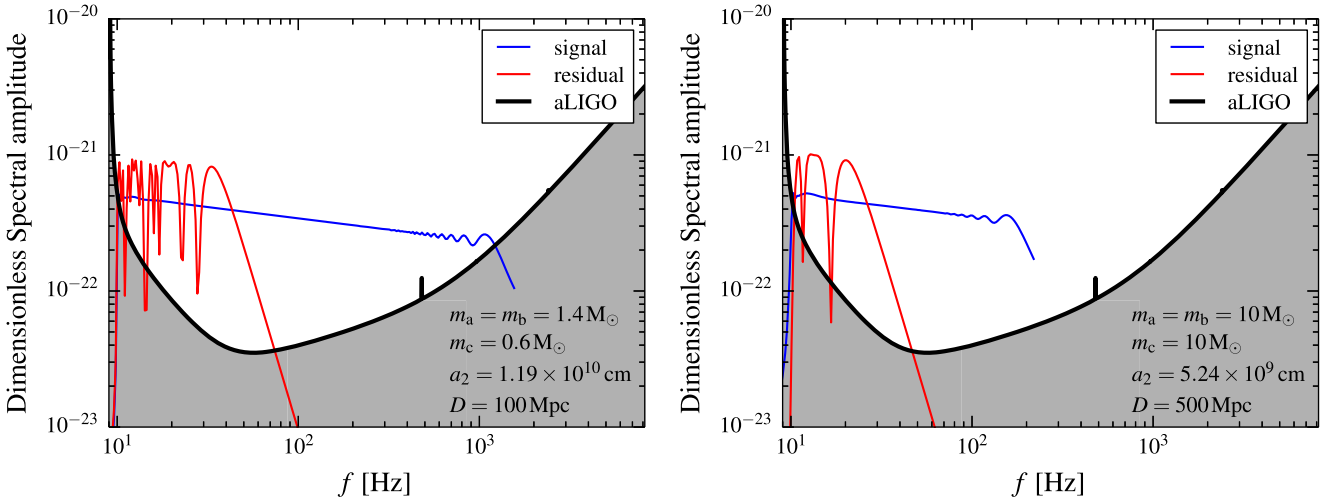

Figure 2. Dimensionless gravitational wave spectral amplitude (blue curve) and root mean square (rms) spectral noise amplitude per logarithmic frequency bin of Advanced LIGO (black curve) from a merging binary system of (left panel) two 1.4 $M_\odot$ neutron stars (NSs) with a 0.6 $M_\odot$ white dwarf companion on a circular orbit at a separation 1.185×10^{10} cm located at a distance of 100 Mpc from the Earth; (right panel) two 10 $M_\odot$ black holes (BHs) with another 10 $M_\odot$ BH companion on a circular orbit at a separation 5.244×10^{9} cm located at a distance of 500 Mpc from the Earth. The red curves show the spectral density of the residual between the signal and a reference signal of a merging binary with no triple companion. The signal progresses in time from left to right; the line ends when the (inner) binary reaches the innermost stable circular orbit. The coalescence and ringdown phases are not shown. The signal-to-noise ratio of (S/N) the signal itself in both examples is ∼14; the residual alone has S/N of 12.5 (NSs) and 7.5 (BHs).

this holds. The distance a_2 where ϕ_2 changes by less than 1 rad while the inner binary is in the LIGO band, from Equation (5), is

$$a_2 \gtrsim \begin{cases} 2.3\, R_\odot \bar{f}_{\rm min}^{-16/9}\, (4\eta_1)^{-2/3} \bar{M}_1^{-7/9} & \text{if } m_c \ll M_1, \\ 2.3\, R_\odot \bar{f}_{\rm min}^{-16/9}\, (4\eta_1)^{-2/3} \bar{M}_1^{-10/9} \bar{m}_c^{1/3} & \text{if } m_c \gg M_1. \end{cases} \quad (20)$$

If this condition is not satisfied, then the outer binary makes a larger revolution during the LIGO measurement than 1 rad, and the simple estimate in Equation (19) becomes inaccurate. For 1 rad outer binary revolution,

$$\delta\Phi_{\rm D}^{(1\,{\rm rad})} \approx \begin{cases} 170 \sin\iota_2\, \bar{f}_{\rm min}^{-7/9}\, (4\eta_1)^{-2/3} \bar{M}_1^{-16/9} \bar{m}_c & \text{if } m_c \ll M_1, \\ 170 \sin\iota_2\, \bar{f}_{\rm min}^{-7/9}\, (4\eta_1)^{-2/3} \bar{M}_1^{-10/9} \bar{m}_c^{1/3} & \text{if } m_c \gg M_1. \end{cases} \quad (21)$$

Furthermore, note that a_2 must be greater than the bound set by the hierarchical triple stability criterion in Equation (8) where $a_1 = 5.1 \times 10^7$ cm $\bar{M}_1^{1/3} \bar{f}_{\rm min}^{-2/3}$ when the inner binary enters the LIGO band (see Equation (1)), and the inner binary must be outside of the ISCO of the outer binary, $a_1 \geqslant a_{2,\rm ISCO}$. Equations (19) and (21) show that GW phase shift due to the third object may be significant for a wide range of parameters.

Figure 3 shows the Doppler phase shift for merging NS–NS and BH–BH binaries as a function of the triple companion distance and mass, by fully numerically solving Equation (17). The black dashed lines show the amount of time the system has been hierarchical and stable as discussed in Section 2, $10^{-3,0,3,6}$ year from left to right, respectively. The black solid line corresponds to 1 rad orbit for the outer binary during the lifetime in the LIGO band for reference (cf. Equation (21)). The region to the left of the black solid line corresponds to systems where the outer binary completes a larger orbital phase during the LIGO measurement. The only LIGO-specific information that enters into this figure is $f_{\rm min} = 10$ Hz, which determined the signal's duration, the phase shift is otherwise independent of detector properties and the source's distance.

Figure 4 shows the S/N of the residual signal for merging NS–NS and BH–BH binaries as a function of the triple companion distance and mass, using the Advanced LIGO sensitivity curve (Shoemaker 2015). The residual signal is the difference between the aforementioned source and reference system. For each pixel in the two panels in the figure, the full time domain waveform is calculated for both source and reference system, Fourier transformed, and integrated according to Equation (16), i.e., without utilizing the stationary phase or the small angle approximations.

4.2. Gravitational Redshift

Another potentially important physical effect that distorts the signal in a triple system is gravitational redshift. In the presence of an additional mass such as that of the triple companion's, the GWs from the inner binary have to climb out of a deeper potential well than in the isolated binary case, and are thus redshifted with respect to the observer, in analogy with electromagnetic radiation in the same situation. This is the result of gravitational time dilation or difference in clock rate, which has an equivalent effect on the GW phase as the difference in "light"-travel time we discussed in Section 4.1.

Since a GW-generating binary of mass M at fixed redshift z may not be distinguishable from an isolated binary with mass $M(1+z)$, the only way gravitational redshift can affect the signal in a measurable way is if the outer binary is eccentric, and the amount of redshift changes along the orbit. Thus, for the reference system we do not choose an isolated binary as in the previous section, but a binary at an arbitrary point along the outer eccentric orbit where the redshift is z_0. The phase difference is thus

$$\delta\Phi_z = \Phi[t_{\rm em}(1 + z(t_{\rm em}))] - \Phi[t_{\rm em}(1 + z_0)], \quad (22)$$

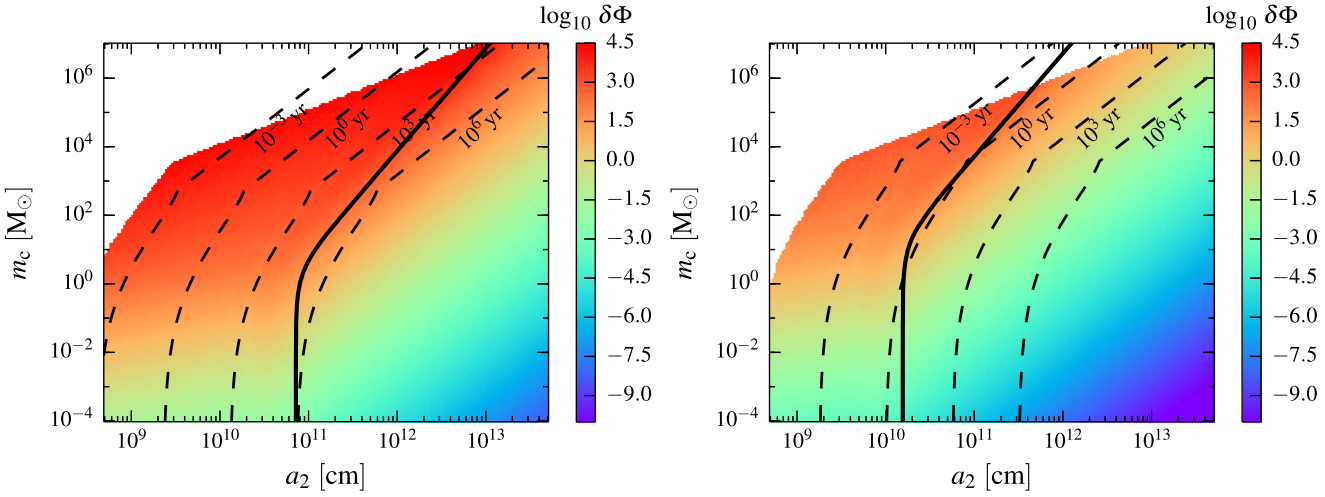

Figure 3. Total Doppler phase shift of the gravitational wave signal compared to a reference waveform, from a merging NS–NS binary (left panel) and a BH–BH binary (right panel) due to a perturber, while the signal is in the LIGO/Virgo frequency band; $\log_{10}\delta\Phi$ is shown as a function of the perturber's distance and mass. For systems along the thick solid line, the outer binary has completed 1 rad of its orbit while the system is in the LIGO band (left of the curve means larger fraction of the orbit). The triple system is unstable in the white region on the top left due to either Newtonian dynamical reasons or the outer separation is smaller than the ISCO; the dashed lines represent the time that the system could have been dynamically stable (i.e., has existed no longer than the amount of time shown on the line). The signal may be detectable if $\log_{10}\delta\Phi \gtrsim 0$ and the source is within the LIGO horizon. The only LIGO-specific information that enters into this figure is $f_{\rm min} = 10$ Hz as it determined the signal's duration, the phase shift is otherwise independent of detector properties and the source's distance.

where $\Phi(t)$ is given by Equation (3) and $z(t_{\rm em})$ is the gravitational redshift of the GW source corresponding to the distance from m_c at source time $t_{\rm em}$. To leading order in the small quantity m_c/a_2 the gravitational redshift is

$$z \approx \frac{m_c}{a_2}\frac{1+e_2\cos\phi_2}{1-e_2^2} = \frac{m_c}{a_2(1-e_2\cos E_2)}, \tag{23}$$

where ϕ_2 is the true anomaly and E_2 is the eccentric anomaly which evolves as $\Omega_2 t = E_2 - \sin E_2$, and we made some simplifying assumptions about the geometry of the system (namely that the eccentricity vector, the angular momentum vector, and the LOS are in the same plane).[16]

If we set $z_0 = z(t_0)$ and substitute Equation (3) in Equation (22), the phase difference between the model including redshift and the one that assumes a constant redshift vanishes at merger by definition. The total phase difference accumlates as a function of time before merger. For the full GW observation, Equation (22) must be evaluated at the point where the signal enters the sensitive frequency band at $f_{\rm min}$. Since z is much less than unity, we may expand Equation (22) to first order around this point to get

$$\begin{aligned}\delta\phi_z &\approx \dot{\Phi} t_{1,\rm merge}\Delta z = f_{\rm min}\, t_{1,\rm merge}\frac{m_c}{a_2}\frac{e_2}{1-e_2^2}\Delta\cos\phi_2 \\ &= 0.74\,\bar{f}_{\rm min}^{-5/3}(4\eta_1)^{-1}\bar{M}_1^{-5/3}\bar{m}_c\bar{a}_2^{-1}\frac{e_2}{1-e_2^2}\Delta\cos\phi_2,\end{aligned} \tag{24}$$

where $\Delta\cos\phi_2$ is the change in $\cos\phi_2$ during the time the source is in the LIGO frequency band (Equation (2)), which is at maximum 2 if it completes half an orbit. If it completes less than 1 rad, we can approximate $|\Delta\cos\phi_2| \approx \Omega_2 t_{1,\rm merge}\sin\phi_{2,0}$ to leading order around $\phi_{2,0}$, which gives

$$\delta\Phi_z \approx \begin{cases} 2.6\chi\,\bar{f}_{\rm min}^{-13/3}(4\eta_1)^{-2}\bar{M}_1^{-17/6}\bar{m}_c\bar{a}_2^{-5/2} & \text{if } m_c \ll M_1, \\ 2.6\chi\,\bar{f}_{\rm min}^{-13/3}(4\eta_1)^{-2}\bar{M}_1^{-10/3}\bar{m}_c^{3/2}\bar{a}_2^{-5/2} & \text{if } m_c \gg M_1, \end{cases} \tag{25}$$

where $\chi = [e_2/(1-e_2^2)]\sin\phi_{2,0}$. The maximum phase shift corresponds to the case where the outer binary completes exactly one half orbit, which implies that

$$\delta\Phi_z \leqslant 1.4\frac{e_2}{1-e_2^2}\bar{f}_{\rm min}^{1/9}(4\eta_1)^{-1/3} \times \begin{cases} \bar{M}_1^{-8/9}\bar{m}_c & \text{if } m_c \ll M_1, \\ \bar{M}_1^{-5/9}\bar{m}_c^{2/3} & \text{if } m_c \gg M_1. \end{cases} \tag{26}$$

This shows that the variation of the gravitational redshift around the perturber is typically smaller than the Doppler phase, but it may still be several radians if the perturber is a BH with $m_c \gtrsim 5\ M_\odot$. Note that $\delta\Phi_z$ is independent of the binary inclination, and it is nonzero only if the perturber is on an eccentric orbit.

4.3. Shapiro Delay

The Shapiro delay is a well known general-relativistic effect that causes the delay in arrival time of a signal when it passes in the gravitational field of a massive object. The time shift caused by the signal propagating in the gravitational field of the perturber is given by Equation (5.5) in Backer & Hellings (1986),

$$\delta t_S = m_c \ln\left|\frac{1+e_2\cos\phi_2}{1-\sin\iota_2\cos(\phi_2+\omega_2)}\right|, \tag{27}$$

where ω_2 is the outer binary's argument of periastron. The corresponding phase shift may be derived similarly to that

[16] If the outer orbits completes more than one revolution in the LIGO band, general relativistic precession may not be neglected.

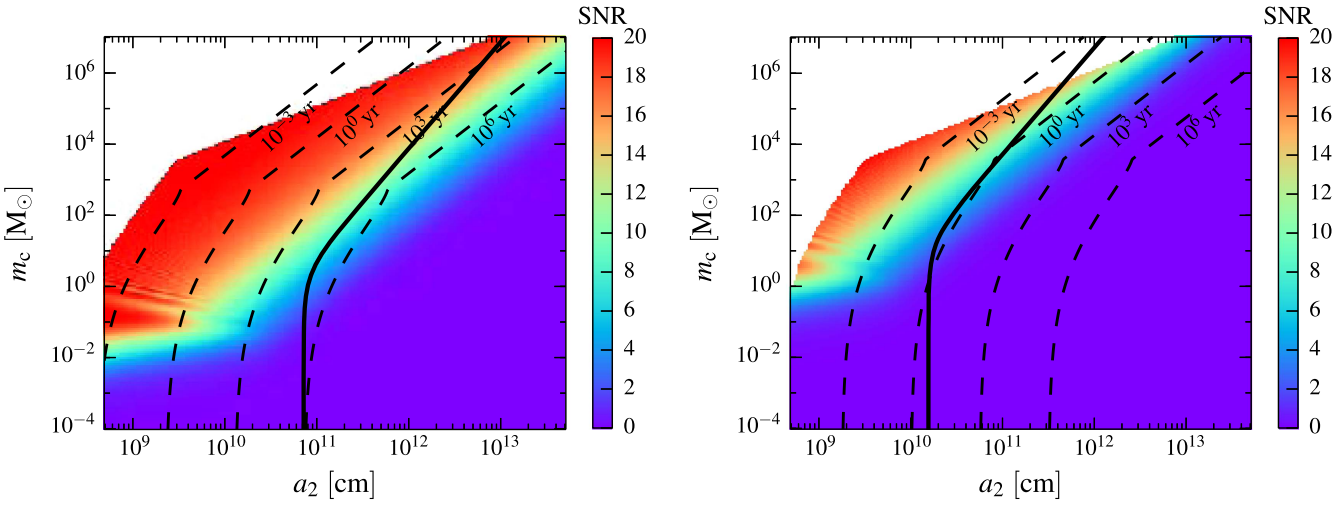

Figure 4. Similar to Figure 3, but now showing the S/N of the residual between the signal and the reference waveform. The Advanced LIGO sensitivity curve is used, and the NS–NS binary (left panel) is put at 100 Mpc from the Earth, while the BH–BH binary (right panel) is put at a distance of 500 Mpc.

presented in Section 4.2, which gives to leading order

$$\delta\Phi_S = \dot{\Phi}\delta t_S = 2\pi f_{\rm min}\,\delta t_S \leqslant 2\pi f_{\rm min}\, m_c|\ln\Lambda| = 3.1\times 10^{-4}\bar{f}_{\rm min}\,\bar{m}_c|\ln\Lambda|, \quad (28)$$

where $\dot{\Phi}$ is the time-derivative of the GW phase given by Equation (3) evaluated at $t = t_{1,\rm merge}$ given by Equation (2), and in the last line we estimated the maximum value of the Shapiro delay assuming a half orbit of the outer binary where

$$\ln\Lambda = \ln\left(\frac{1+e_2}{1-e_2}\right) + \ln\left(\frac{1-\sin\iota_2}{1+\sin\iota_2}\right). \quad (29)$$

The expectation value for thermally distributed eccentricities[17] and isotropically distributed inclinations is $\langle|\ln\Lambda|\rangle = 2$. This expression shows that $\delta\Phi_S$ is typically much less than 1 rad unless $m_c \gtrsim 10^3\,M_\odot$ or if the outer binary is almost exactly edge on. The Doppler shift and the gravitational redshift typically cause larger perturbations.

4.4. Dynamical Effects

In the above sections, the waveform emitted by the binary was intrinsically unchanged by the presence of the perturber; the GW signal observed on the Earth was distorted due to the change of frame of reference. Now we examine the dynamical torque generated by the triple companion which may change the orbital elements of the inner binary. The leading-order dynamical perturbation is the quadrupole component of the tidal gravitational field of the perturber (Will 2014). This leads to both oscillatory variations on the inner orbit timescale and a secular change in the eccentricity and angular momentum vector on much longer timescales, discussed next (see Galaviz & Brügmann 2011; Naoz et al. 2013b, for further post-Newtonian dynamical three body effects for eccentric triples).

4.4.1. Nodal Precession

If the inner and outer binaries are not in the same plane, the angular momentum and eccentricity vectors of the inner binary undergo long-duration changes. For a circular inner binary, the angular momentum of the inner binary $\boldsymbol{L}_1$ precesses around the total angular momentum $\boldsymbol{L}_{\rm tot} = \boldsymbol{L}_1 + \boldsymbol{L}_2$. The corresponding nodal precession rate to leading Newtonian quadrupole order is (Naoz et al. 2013a, 2013b)

$$\Omega_{1,\rm nodal} = \frac{3}{4}\frac{m_c}{M_1}\Omega_1\frac{a_1^3}{a_2^3}\frac{L_{\rm tot}}{L_2}\frac{\cos\theta}{(1-e_2^2)^{3/2}}, \quad (30)$$

where $\Omega_1 = \pi f$, $a_1 = M_1(\pi M_1 f)^{-2/3}$ is the angular frequency and

$$\boldsymbol{L}_i = \eta_i M_i^{3/2}(1-e_i^2)^{1/2}\hat{\boldsymbol{L}}_i \quad (31)$$

for binary i, $\hat{\boldsymbol{L}}_i$ is a unit vector, $L_i = \|\boldsymbol{L}_i\|$, and $\cos\theta = \hat{\boldsymbol{L}}_1\cdot\hat{\boldsymbol{L}}_2$. The orbital plane precession angle is set by

$$\delta\varphi = \frac{L_2}{L_{\rm tot}}\Omega_{1,\rm nodal}\,t_{1,\rm merge} = 5.2\times 10^{-5}\,\bar{f}^{-11/3}\bar{M}_1^{-5/3}m_c\bar{a}_2^{-3}\frac{\cos\theta}{(1-e_2^2)^{3/2}}. \quad (32)$$

Secular precession effects are therefore expected to be significant if $a_2 \lesssim 0.1\,R_\odot$ for stellar mass perturbers or if $a_2 \lesssim 1\,R_\odot$ for intermediate or supermassive BH perturbers.

4.4.2. Change in the Orbital Shape

The tidal force of the perturber acting on the binary due to the triple companion affects the orbital shape similar to how the Moon raises ocean tides on Earth. In a corotating frame with angular velocity Ω_1 with the inner binary, the Newtonian equations of motion become

$$\ddot{\boldsymbol{r}}_1 = \Omega_1^2\boldsymbol{r}_1 - 2\,\boldsymbol{\Omega}_1\times\dot{\boldsymbol{r}}_1 - \frac{M_1}{r_1^3}\boldsymbol{r}_1 - \frac{m_c}{r_2^3}\boldsymbol{r}_1 + 3\frac{m_c(\boldsymbol{r}_1\cdot\boldsymbol{r}_2)}{r_2^5}\boldsymbol{r}_2, \quad (33)$$

where $\boldsymbol{r}_i$ is the separation vector of the ith binary, the first two terms are the centrifugal and Coriolis forces for a coplanar triple, and the last two are the tidal force. The mean orbital frequency is modified by the fourth term, and the last term introduces a time-dependent perturbation to the orbital shape. If the unperturbed orbit is approximately circular, the acceleration in the $\boldsymbol{r}_2$ direction due to the last term is on average $\frac{3}{2}m_c r_1/r_2^3$.

[17] Note that e_2 may not approach unity since that would lead to disruption of the inner binary.

Assuming a constant acceleration of this magnitude in this direction for a half-period duration, π/Ω_1, we may estimate the corresponding distance traveled, and the corresponding orbital eccentricity:

$$e_1 \sim \frac{\Delta r_1}{r_1} \sim \frac{1}{2} \times \frac{3}{2}\frac{m_c}{r_2^3} \times \left(\frac{\pi}{\Omega_1}\right)^2 = 10^{-10}\bar{f}^{-2}\bar{m}_c\bar{r}_2^{-3}. \quad (34)$$

The orbital eccentricity also changes the shape of the GW waveform. If a corresponding phase shift is of order $\delta\Phi \sim e_1\Phi$, this may be significant for LIGO/Virgo if $r_2 \lesssim 0.1\,R_\odot$ for stellar mass perturbers or $r_2 \lesssim R_\odot$ for $m_c \gg 10^4\,M_\odot$. Note that $\Phi \sim 5.6 \times 10^5 \bar{f}^{-5/3}(4\eta_1)^{-1}\bar{M}_1{}^{-5/3}$ according to Equation (3).

5. DISCUSSION

5.1. Summary of Results

We have shown that Advanced LIGO/Virgo is capable of identifying a third object in the vicinity of a compact object merger by detecting its imprint on the GW waveform. The most prominent perturbation of the third object is due to the time-varying path length to the source (the Doppler phase) as the source orbits around the perturber. Second, the effects of a time-dependent gravitational redshift due to the third object is also significant in many cases. The Shapiro delay may be detectable for intermediate mass (IMBH) or supermassive (SMBH) BH perturbers beyond $10^3\,M_\odot$. Dynamical effects of the third object on the orbital elements of the merging binary are less important for circular inspirals unless the pertuber distance is much less than a solar radius.

The GW Doppler phase may well exceed a radian for a wide range of perturber masses and distances (Figure 3). For circular NS–NS binaries, a stellar mass compact object companion causes a significant Doppler GW phase shift if it is within a few solar radii ($\sim 10^{11}$ cm) to the binary and a $10^6\,M_\odot$ SMBH companion causes a significant Doppler phase if it is within a few astronomical units ($\sim 10^{13}$ cm). For circular stellar BH–BH binaries the third companion must be a factor $\sim$10 closer to drive a similar Doppler phase shift (Equation (19)), mainly because the binaries spend a shorter amount of time in the LIGO/Virgo frequency band (i.e., 16 minutes for circular NS–NS and tens of seconds for circular BH–BH binaries). For these parameters, the effect of the triple companion may be detected in the GW signal as shown by Figure 4 provided that the GW source is within the LIGO/Virgo horizon (e.g., S/N $\gtrsim$ 8 for the unperturbed inspiraling binary).

5.2. Event Rates and Electromagnetic Counterparts

The likelihood of discovering such triple systems is currently not well constrained by theoretical models. It is well known that a large fraction of massive stars are in triples (see Section 1), which may be progenitors of compact object triples detectable by LIGO/Virgo. However, for known systems, the third object is at a much wider separation than a few solar radii necessary for LIGO/Virgo detection (Ransom et al. 2014). The maximum lifetime of close stellar mass compact object triple systems detectable by LIGO/Virgo is limited by stability arguments and GW emission to within a few Myr (see dashed lines in Figures 3 and 4). These stellar-mass triple systems may form dynamically in dense stellar systems where the encounter rate is high, such as in the cores of globular clusters. Alternatively, an SMBH perturber to a LIGO event may be detected to somewhat larger distances, a few astronomical units (Figure 4). However most compact object binaries are expected to reside at much larger distances from SMBHs in stellar cusps (Pfuhl et al. 2014; Stephan et al. 2016). The maximum lifetime of these binaries at distances where the SMBH may be detected due to GW emission is a few Myr, similar to stellar-mass perturbers (Figures 3 and 4). Binaries falling to the vicinity of an SMBH may merge due to secular Kozai–Lidov oscillations excited by the SMBH (Antonini & Perets 2012).

One plausible way to form such tight compact object triples is in AGNs. Compact object binaries may get captured by an accretion disk of an SMBH or form therein. In this case, the SMBH around the binary represents the triple companion. The interaction of the binary with the gaseous disk transports the inner binary close to the SMBH, aligns the orbital planes, and drives the inner binary to merge (Bartos et al. 2016; Stone et al. 2016). These authors estimate the event rates for these mergers inside disks at around a few tens of detections per year for Advanced LIGO/Virgo, but this estimate is highly uncertain (also note that the triple companion, in this case the SMBH, may not be observable in many of these merger events). The vicinity of the SMBH may be possibly detected through the Doppler GW phase with LIGO/Virgo if they migrate to within a thousand gravitational radii of the SMBH. Further in this case, a GW echo may also be possibly detected due to the SMBH (Kocsis 2013). Detecting an SMBH triple companion with an aligned orbit with the inner binary may be a smoking gun to infer the presence of an AGN accretion disk in the vicinity of the GW source. Since an inclined outer binary drives nodal precession, an analysis of the GW perturbation driven by the companion may allow one to identify the relative inclination of the inner and outer binaries. The relative inclination may also be measured directly by detecting the GWs of the outer binary with *LISA* in coincidence (see Section 5.3).

An attractive property of these GW sources is that they have electromagnetic counterparts. The accretion disks of AGNs are visible to cosmological distances with electromagnetic telescopes and they are much less common than galaxies or globular clusters, which allows us to cut down on the possible counterpart candidates to the GW event (Kocsis et al. 2006, 2008).

Furthermore, a massive progenitor star with a short-period compact object binary companion may form a stellar-mass compact object triple detectable by LIGO/Virgo. The collapse of a massive star may form a compact object *inner binary*, which merges due to GW emission (Kinugawa et al. 2014). In this case, the outer object would become the triple companion which leaves its imprint on the GWs of this inner binary. In this case, the collapse of the massive star forming the inner binary might appear as a supernova explosion or a gamma-ray burst (Reisswig et al. 2013; Dvorkin et al. 2016; Loeb 2016; Woosley 2016).

While our estimates were limited to circular-inspiraling inner binaries, we note that triple companions to eccentric inner binaries may be common. The inspiral time of eccentric binaries within the LIGO/Virgo frequency band may be a factor $\sim$100$\times$ longer, especially in the highly eccentric, the so-called repeated burst phase (O'Leary et al. 2009; Kocsis & Levin 2012). For these systems, the triple companion may be at a much larger separation for the binary to execute a significant orbital phase around the triple's center of mass and to cause a

significant Doppler GW phase shift for the inner binary signal. Thus, the lifetime of such triples may be much longer, and so the likelihood of detectable triples in LIGO/Virgo mergers might be expected to be much more common among eccentric LIGO/Virgo sources. Further, since GW emission tends to decrease the eccentricity as it shrinks the pericenter distance down to merger, the eccentricity may commonly be significant during earlier stages of the inspiral when the GW signal is in the *LISA* frequency band (see Section 5.3). Dynamical perturbations of the triple companion may be significant for these sources (Section 4.4). Post-Newtonian interaction terms involving all three objects may possibly be detected, which could provide a new test of general relativity (Naoz et al. 2013b; Will 2014). We leave a detailed investigation of eccentric triple GW sources to future work.

5.3. Multiband GW Detections

Since detecting the presence of a third companion to a merger is primarily limited by the time duration that the binary spends in the detector's sensitive frequency band, the likelihood of identifying triples may be greatly increased for future GW detectors by decreasing their minimum frequency threshold. Note that the phase shift due to the triple companion scales steeply as $f_{\rm min}^{-13/3}$ to leading order (Equation (19)). Ultimately, *LISA* will be the best suited to identify stellar mass triples, since here the orbital time of the inner binary may be several years in the detectable frequency band. Note that binaries like GW150914 could be detected at $S/N \sim 10$ by *LISA* years before merger (Sesana 2016), and triple companions with orbital periods of years may be possibly discovered for those mergers.

Is there any other independent way to detect the triple companion in the vicinity of a LIGO/Virgo source? The orbital frequency of the outer binary, for high S/N LIGO/Virgo detections, must be comparable to or higher than the inverse merger time of the inner binary in the LIGO/Virgo frequency band (see thick solid line in Figures 3 and 4). This is 10^{-3} Hz for NS–NS and 0.02 Hz for BH–BH binaries, which is well within the sensitive frequency band for *LISA*. Therefore, while the inner binary merges in the LIGO/Virgo band, the *outer binary* may be coincidentally detected by *LISA*. Further, if the outer binary seperation is sufficiently small, the outer binary itself may merge within a few years following the inner binary merger, which may be detectable with LIGO/Virgo if the companion mass is less than $10^3\,M_\odot$. Such spectacular detection sequences may allow for a very accurate parameter estimate determination for these triple systems.

A possible example of such a system is shown in Figure 5, where a $8\,M_\odot + 8\,M_\odot$ BH–BH circular inner binary is accompanied by a $20\,M_\odot$ BH on a $0.1\,R_\odot$-separation circular outer orbit, 100 Mpc from the Earth. If this triple system was circular throughout its prior evolution, then it must have formed within 7 days prior to the inner's merger due to the stability arguments presented in Section 2. Thus, the formation of the triple should be captured by *LISA*, as well as the outer binary's inspiral during this phase. This is followed by a detection of the merger event by both *LISA* and LIGO/Virgo (the total Doppler GW phase shift is 5.8 rad). Due to the GW recoil kick and a sudden mass loss in the merger process of the inner binary, the outer binary's linear momentum, eccentricity, and inclination suddenly change, leaving an imprint on the outer binary's GW waveform (not shown in the figure) measurable by *LISA*. Following the inner binary coalescence, the inner remnant BH and the outer BH inspirals as an isolated binary, leaving the *LISA* band while continuing to circularize and shrink for 7 years, before showing up in the LIGO/Virgo band and merging.

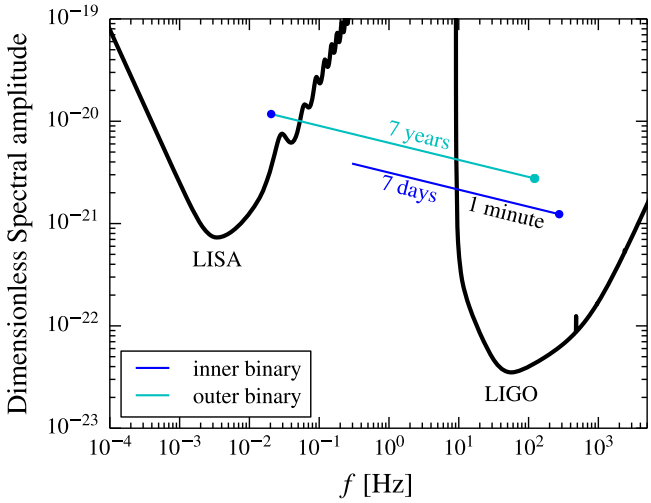

Figure 5. Dimensionless spectral amplitude due to a triple system comprised of a circular inner binary of two $8\,M_\odot$ BHs and a $20\,M_\odot$ companion BH, at a distance of 100 Mpc. The inner binary is in the LIGO band for 55 s, during which the triple companion induces a Doppler shift $\delta\Phi$ of 5.8 rad. Stability analysis shows that such a circular system must have formed in at most 6.9 days before the inner binary signal was detected with LIGO. The GW frequency of the outer binary is in the *LISA* band during the LIGO detection. Following the inner binary merger, the outer binary GW frequency leaves the *LISA* band and 6.7 years later enters the LIGO band. The filled blue circles represent the ISCO of the inner binary, the cyan circle represents the ISCO of the outer binary (the ringdown is not shown for either binary).

5.4. Search Techniques and Degeneracies

Finally, we comment on some practical issues related to data analysis and GW detections. While the number of parameter to describe a binary is generally[18] 17, the number of parameters to fully characterize a hierarchical BH triple system is 27 due to the mass, six orbital elements, and three spin vector components of the perturber. This may seem to be dauntingly high to carry out a full template-based search for these waveforms. Fortunately, there are several points suggesting that this task may not be impossible. First, the three spin components of the third companion do not affect the evolution of the inner binary in any measurable way if the separation is $a_2 \gg 10^3\ M_2$, since spin effects are higher post-Newtonian order (1.5 PN) (Apostolatos et al. 1994). Second, most of the seven parameters of the triple companion will be degenerate with respect to their effects on the inner binary waveform. For instance, the leading order perturbation, the Doppler phase shift at frequency f (Equation (19)) is set by the LOS acceleration as $\delta\Phi_{\rm D} \propto f^{-10/3}\dot{v}_{1,\rm los}$ approaching merger, where $\dot{v}_{1,\rm los}$ is approximately constant (Yunes et al. 2011b). The remaining effects are typically much smaller approaching merger. Due to the wide hierarchy in the perturbation effects $\delta\Phi_{\rm D} \gg \delta\Phi_{\rm z} \gg \delta\Phi_{\rm S}$, and different frequency dependence of these effects, there is room to optimize search algorithms to identify the leading order

[18] I.e., nine parameters for circular orbits with nonspinning components, six spin parameters, and two parameters for eccentric orbits.

perturbations of triples as an alternative to a brute force template-based search.

Importantly, we argue that search algorithms may identify the merging inner binary even if completely neglecting all of the perturbation of the triple. The frequency scaling relations (Equations (15) and (19)) yield $\delta\Phi_{\rm D}/\Psi = f^{-8/3}$, hence the perturbation is typically negligible at high frequencies approaching the ISCO, and it accumulates to any substantial level only at much lower frequencies. Indeed, Figure 2 confirms that the perturbation has a significant S/N per logarithmic frequency interval at frequencies well below the ISCO. The mismatch between an isolated binary waveform and a binary with a triple companion may become significant only below 50 Hz (Figure 2). A systematic dephasing at low frequencies could be a sign of a third companion.

Fortunately, the frequency dependence of the Doppler phase has the opposite trend than post-Newtonian corrections which *increase* as a function of f. In other words, the mass ratio and the spin effects get significantly larger when approaching merger, while the effect of a third companion does not. Therefore, the general expectation is that these effects probably cannot mimic the effect discussed in this paper in the limit of a high S/N and several triple cycles. However, if the S/N is not high enough, or if the outer binary completes much less than 1 rad of its orbit, then the perturbation may be confused by variations of the other parameters. The same statement cannot be made for residual eccentricity of an isolated binary; further study is needed to determine whether it could be confused with the waveform from a circular inner binary in a triple system. Additionally, the leading order triple companion effects on the waveform may be degenerate with isolated binary waveforms that incorporate possible modifications to the theory of general relativity (Abbott et al. 2016d; Yunes et al. 2016).

This work was supported in part by the European Research Council under the European Union's Horizon 2020 Programme, ERC-2014-STG grant GalNUC 638435 and by NSF grant AST-1312034. The calculations were carried out on the NIIF HPC cluster at the University of Debrecen, Hungary.

REFERENCES

Abbott, B. P., Abbott, R., Abbott, T. D., et al. 2016a, PhRvL, 116, 061102
Abbott, B. P., Abbott, R., Abbott, T. D., et al. 2016b, arXiv:1602.03842
Abbott, B. P., Abbott, R., Abbott, T. D., et al. 2016c, PhRvD, 93, 122003
Abbott, B. P., Abbott, R., Abbott, T. D., et al. 2016d, PhRvD, 116, 221101
Alic, D., Moesta, P., Rezzolla, L., Zanotti, O., & Jaramillo, J. L. 2012, ApJ, 754, 36
Amaro-Seoane, P., & Chen, X. 2016, MNRAS, 458, 3075
Antognini, J. M., Shappee, B. J., Thompson, T. A., & Amaro-Seoane, P. 2014, MNRAS, 439, 1079
Antonini, F., Murray, N., & Mikkola, S. 2014, ApJ, 781, 45
Antonini, F., & Perets, H. B. 2012, ApJ, 757, 27
Apostolatos, T. A., Cutler, C., Sussman, G. J., & Thorne, K. S. 1994, PhRvD, 49, 6274
Backer, D. C., & Hellings, R. W. 1986, ARA&A, 24, 537
Barausse, E., Cardoso, V., & Pani, P. 2014, PhRvD, 89, 104059
Barausse, E., & Rezzolla, L. 2008, PhRvD, 77, 104027
Bartos, I., Kocsis, B., Haiman, Z., & Márka, S. 2016, arXiv:1602.03831
Belczynski, K., Holz, D. E., Bulik, T., & O'Shaughnessy, R. 2016, arXiv:1602.04531
Bird, S., Cholis, I., Muñoz, J. B., et al. 2016, arXiv:1603.00464
Blaes, O., Lee, M. H., & Socrates, A. 2002, ApJ, 578, 775
Bode, T., Bogdanović, T., Haas, R., et al. 2012, ApJ, 744, 45
Clesse, S., & García-Bellido, J. 2016, arXiv:1603.05234
Cutler, C., & Flanagan, É. E. 1994, PhRvD, 49, 2658
de Mink, S. E., & Mandel, I. 2016, MNRAS, 460, 3553
Dvorkin, I., Vangioni, E., Silk, J., Uzan, J.-P., & Olive, K. A. 2016, MNRAS, 461, 3877
Eggleton, P., & Kiseleva, L. 1995, ApJ, 455, 640
Farris, B. D., Duffell, P., MacFadyen, A. I., & Haiman, Z. 2015, MNRAS, 447, L80
Farris, B. D., Gold, R., Paschalidis, V., Etienne, Z. B., & Shapiro, S. L. 2012, PhRvL, 109, 221102
Galaviz, P., & Brügmann, B. 2011, PhRvD, 83, 084013
Generozov, A., & Haiman, Z. 2014, MNRAS, 443, L64
Giacomazzo, B., Baker, J. G., Miller, M. C., Reynolds, C. S., & van Meter, J. R. 2012, ApJL, 752, L15
Gold, R., Paschalidis, V., Etienne, Z. B., Shapiro, S. L., & Pfeiffer, H. P. 2014a, PhRvD, 89, 064060
Gold, R., Paschalidis, V., Ruiz, M., et al. 2014b, PhRvD, 90, 104030
Hartwig, T., Volonteri, M., Bromm, V., et al. 2016, MNRAS, 460, L74
Inayoshi, K., Kashiyama, K., Visbal, E., & Haiman, Z. 2016, MNRAS, 461, 2727
Ivanova, N., Belczynski, K., Fregeau, J. M., & Rasio, F. A. 2005, MNRAS, 358, 572
Katz, B., Dong, S., & Malhotra, R. 2011, PhRvL, 107, 181101
Kinugawa, T., Inayoshi, K., Hotokezaka, K., Nakauchi, D., & Nakamura, T. 2014, MNRAS, 442, 2963
Kinugawa, T., Miyamoto, A., Kanda, N., & Nakamura, T. 2016, MNRAS, 456, 1093
Kocsis, B. 2013, ApJ, 763, 122
Kocsis, B., Frei, Z., Haiman, Z., & Menou, K. 2006, ApJ, 637, 27
Kocsis, B., Haiman, Z., & Loeb, A. 2012, MNRAS, 427, 2680
Kocsis, B., Haiman, Z., & Menou, K. 2008, ApJ, 684, 870
Kocsis, B., & Levin, J. 2012, PhRvD, 85, 123005
Kocsis, B., & Loeb, A. 2008, PhRvL, 101, 041101
Kocsis, B., & Sesana, A. 2011, MNRAS, 411, 1467
Kocsis, B., Yunes, N., & Loeb, A. 2011, PhRvD, 84, 024032
Li, G., Kocsis, B., & Loeb, A. 2012, MNRAS, 425, 2407
Loeb, A. 2016, ApJL, 819, L21
Mandel, I., & de Mink, S. E. 2016, MNRAS, 458, 2634
Marchant, P., Langer, N., Podsiadlowski, P., Tauris, T., & Moriya, T. 2016, A&A, 588, A50
McKernan, B., Ford, K. E. S., Kocsis, B., & Haiman, Z. 2013, MNRAS, 432, 1468
McKernan, B., Ford, K. E. S., Kocsis, B., & Haiman, Z. 2014, MNRAS, 445, L74
Miller, M. C., & Hamilton, D. P. 2002, ApJ, 576, 894
Naoz, S. 2016, ARA&A, 54, 441
Naoz, S., Farr, W. M., Lithwick, Y., Rasio, F. A., & Teyssandier, J. 2013a, MNRAS, 431, 2155
Naoz, S., Kocsis, B., Loeb, A., & Yunes, N. 2013b, ApJ, 773, 187
Noble, S. C., Mundim, B. C., Nakano, H., et al. 2012, ApJ, 755, 51
O'Leary, R. M., Kocsis, B., & Loeb, A. 2009, MNRAS, 395, 2127
O'Leary, R. M., Meiron, Y., & Kocsis, B. 2016, ApJL, 824, L12
O'Leary, R. M., Rasio, F. A., Fregeau, J. M., Ivanova, N., & O'Shaughnessy, R. 2006, ApJ, 637, 937
Palenzuela, C., Lehner, L., & Liebling, S. L. 2010, Sci, 329, 927
Peters, P. C. 1964, PhRv, 136, 1224
Pfuhl, O., Alexander, T., Gillessen, S., et al. 2014, ApJ, 782, 101
Portegies Zwart, S. F., & McMillan, S. L. W. 2000, ApJL, 528, L17
Pribulla, T., & Rucinski, S. M. 2006, AJ, 131, 2986
Ransom, S. M., Stairs, I. H., Archibald, A. M., et al. 2014, Natur, 505, 520
Reisswig, C., Ott, C. D., Abdikamalov, E., et al. 2013, PhRvL, 111, 151101
Rodriguez, C. L., Morscher, M., Wang, L., et al. 2016, MNRAS, 463, 2109
Roedig, C., Krolik, J. H., & Miller, M. C. 2014, ApJ, 785, 115
Samsing, J., MacLeod, M., & Ramirez-Ruiz, E. 2014, ApJ, 784, 71
Sasaki, M., Suyama, T., Tanaka, T., & Yokoyama, S. 2016, PhRvL, 117, 061101
Schnittman, J. D. 2010, ApJ, 724, 39
Sesana, A. 2016, PhRvL, 116, 231102
Seto, N. 2013, PhRvL, 111, 061106
Seto, N., & Muto, T. 2011, MNRAS, 415, 3824
Shoemaker, D. 2015, LIGO document LIGO-T0900288-v3, https://dcc.ligo.org/LIGO-T0900288/public
Stephan, A. P., Naoz, S., Ghez, A. M., et al. 2016, MNRAS, 460, 3494
Stone, N. C., Metzger, B. D., & Haiman, Z. 2016, MNRAS, 464, 946
Tanaka, T. L., & Haiman, Z. 2013, CQGra, 30, 224012
Tauris, T. M., & van den Heuvel, E. P. J. 2014, ApJL, 781, L13
Tokovinin, A. A. 1997, AstL, 23, 727
Wen, L. 2003, ApJ, 598, 419
Will, C. M. 2014, PhRvD, 89, 044043

Woosley, S. E. 2016, ApJL, 324, L10
Yamada, K., Tsuchiya, T., & Asada, H. 2015, PhRvD, 91, 124016
Yunes, N., Kocsis, B., Loeb, A., & Haiman, Z. 2011a, PhRvL, 107, 171103
Yunes, N., Miller, M. C., & Thornburg, J. 2011b, PhRvD, 83, 044030
Yunes, N., Yagi, K., & Pretorius, F. 2016, PhRvD, 94, 084002
Zhou, T.-Y., Cao, W.-G., & Xie, Y. 2016, PhRvD, 93, 064065